Algal Research 93 (2026) 104466

Contents lists available at ScienceDirect

Algal Research

journal homepage: www.elsevier.com/locate/algal

Morphological response of *Arthrospira platensis* to cultivation conditions using a microfluidic microscope

R. Gomez Vico [a], David-A. Mendels [b], Agathe Nguyen [c], M. Barceló-Villalobos [a], F.G. Acién [a,*]

[a] Department of Chemical Engineering, CEIA3, CIESOL, Ctra. Sacramento s/n, University of Almería, Almería, Spain
[b] Zorth SARL, Aix-en-Provence, France
[c] CentraleSupélec, Joliot-Curie Bâtiment Eiffel/DE/BFE, 91190, Gif-sur-Yvette, France

ARTICLE INFO

Keywords:
A. platensis
Microfluidic microscopy
Biomass monitoring
Filament morphology
Cultivation parameters
AI-based image analysis

ABSTRACT

Arthrospira platensis is a filamentous cyanobacterium valued for its high protein content and biotechnological versatility. This study explores the influence of key environmental parameters—temperature, pH, irradiance, and agitation—on both the morphological characteristics and biomass productivity of *A. platensis*. Using Microdeep™, a novel AI-integrated microfluidic microscope, filament traits such as length, diameter, and structural integrity were quantified alongside dry mass equivalent (DME), serving as a proxy for biomass concentration. Optimal growth conditions were identified at 40 °C, pH 9–10, and an irradiance of 200 μmol·m^{-2}·s^{-1}, under which cultures exhibited maximal filament elongation and biomass yield without structural degradation. Across experimental conditions, filament lengths ranged from 30 to 420 μm and diameters from 6 to 11 μm, highlighting dynamic morphological plasticity. Under adverse conditions—extreme pH (6 or 11), high irradiance (2200 μmol·m^{-2}·s^{-1}), or non-optimal temperatures (10 or 45 °C)—filaments experienced fragmentation, reduced elongation, and biomass decline, primarily driven by stress-induced necridia formation and photodamage. The Microdeep™ system demonstrated a high degree of accuracy in biomass estimation, with dry matter equivalent measurements showing a linear correlation to gravimetric dry weight ($R^2 > 0.99$). This confirms its suitability for real-time cultivation monitoring and opens avenues for precision-controlled photobioreactor operations. Overall, the study reinforces the utility of AI-enhanced imaging tools in optimizing microalgal bioprocesses through detailed, quantitative analysis of morphological and physiological traits.

1. Introduction

Arthrospira platensis, commonly known as Spirulina, is a filamentous cyanobacterium renowned for its exceptional nutritional and biotechnological properties. Nutritionally, *A. platensis* contains 50–75 % protein by dry weight, alongside essential polyunsaturated fatty acids such as linoleic and linolenic acids, B-complex vitamins, vitamins C, D, E, and bioactive pigments like phycocyanin—traits that have led to its classification as a "superfood" [1,2]. A study published in the Journal of the Science of Food and Agriculture emphasized its value as one of the richest microbial protein sources, with protein yields ranging from 460 to 630 g·kg^{-1} dry weight, and highlighted the importance of developing effective extraction strategies for biorefinery processes [3]. Economically, the global production of Spirulina reached approximately 18,000 t in 2023, with a market value estimated at US$577 million and a projected compound annual growth rate (CAGR) of 9.3 % extending through 2032 [4].

To date, the vast majority of commercial *A. platensis* cultivation is performed in open raceway systems, with culture volumes ranging from 10 to 1000 m^3 [5,6]. In these settings, mechanical paddle wheels are commonly employed to ensure adequate mixing and homogenization of the culture [7]. Open raceways are widely favored for their simple design, ease of operation, and low capital and operational costs [5]. However, this approach is not without limitations. Open systems are particularly vulnerable to biological contamination by protozoa, competing microalgae, and pathogenic bacteria, as well as to chemical contamination from external sources [8].

A. platensis thrives in alkaline-saline conditions (optimal pH 9–10), which naturally inhibit the growth of many contaminant organisms. This ecological advantage, coupled with the organism's high photosynthetic efficiency and resilience under environmental stress, makes it highly suitable for cultivation in marginal lands and circular-resource

* Corresponding author.
E-mail address: facien@ual.es (F.G. Acién).

https://doi.org/10.1016/j.algal.2025.104466
Received 10 July 2025; Received in revised form 20 October 2025; Accepted 3 December 2025
Available online 5 December 2025

systems [1,2]. Morphologically, *A. platensis* forms helical, multicellular filaments typically measuring 50–500 μm in length and 6–12 μm in diameter [1]. It reproduces via binary fission, during which necridia—segments that facilitate filament division—preserve genetic continuity while enhancing population expansion [9]. This robust filamentous structure is essential for efficient biomass harvesting, as it supports mechanical stability and maintains yield quality throughout downstream processes.

From a bioprocessing standpoint, the morphology of *A. platensis*—particularly filament length, spiral integrity, and biomass density—is a critical determinant of both harvestability and biomass quality. Structurally robust filaments not only improve separation efficiency during harvesting but also reflect a physiologically healthy culture state conducive to high productivity [10]. Morphological features are highly responsive to environmental cues such as temperature, pH, irradiance, and shear stress, making them sensitive indicators of the culture's physiological status [11,12].

For example, elevated temperatures may accelerate cell metabolism and division but can also lead to increased filament fragmentation or spiral unwinding, especially when exceeding the optimal thermal range [12]. Similarly, extreme pH values—both acidic and highly alkaline—can destabilize cell wall integrity and promote necridia formation, a phenomenon associated with filament breakage and stress responses [9]. Light intensity also plays a dual role: while moderate irradiance enhances biomass accumulation and elongation of filaments, excessive irradiance induces photodamage, resulting in shortened and degraded filaments [13].

Despite these dynamic morphological responses, most industrial systems rely on bulk optical parameters such as optical density or chlorophyll fluorescence to estimate growth, which often overlook structural changes occurring at the cellular level [14]. Incorporating real-time morphological analysis into cultivation workflows could serve as an early diagnostic tool to detect suboptimal conditions and forecast declines in culture productivity before they become apparent through bulk metrics. Hence, morphology not only correlates with immediate harvestability but also serves as a functional proxy for overall culture health and performance.

In this context, the present study investigates the morphological response of *A. platensis* to variations in key cultivation parameters—including temperature, pH, irradiance, and agitation—using a novel microfluidic imaging system known as Microdeep™. This platform combines real-time optical imaging with artificial intelligence to automatically analyze critical morphological features such as filament length, diameter, and integrity, alongside quantifying biomass through dry matter equivalent (DME). Unlike traditional bulk measurements like optical density or chlorophyll content, the Microdeep™ system enables high-resolution, population-scale analysis of structural traits, offering deeper insights into culture health and dynamics [15].

The main objective of this study is to determine how different environmental factors shape filament morphology and biomass productivity, using DME as a real-time, image-based proxy for dry weight concentration. By integrating morphological and physiological data, this approach enables the development of more precise, responsive control strategies for large-scale photobioreactor systems. AI-powered monitoring tools such as Microdeep™ thus offer a significant advancement toward the automation and optimization of microalgal bioprocesses, especially in applications aiming for high-value biomass and reduced operational risks [10,14].

2. Materials and methods

2.1. Microorganism and culture medium

The microalgal strain used in this study was *A. platensis*, provided by Algaria (Italy). Cultivation was conducted in a modified Arnon medium designed to support optimal growth conditions for filamentous cyanobacteria. The medium was enriched with sodium bicarbonate and sodium nitrate as primary carbon and nitrogen sources, respectively, while conventional micronutrient solutions were replaced by Karentol, a commercial trace element mix. The complete composition of the culture medium per litre of distilled water was as follows: 16.8 $g{\cdot}L^{-1}$ $NaHCO_3$, 0.85 $g{\cdot}L^{-1}$ $NaNO_3$, 0.174 $g{\cdot}L^{-1}$ K_2HPO_4, 0.124 $g{\cdot}L^{-1}$ $MgSO_4{\cdot}7H_2O$, 0.015 $g{\cdot}L^{-1}$ $CaCl_2{\cdot}2H_2O$, 0.117 $g{\cdot}L^{-1}$ NaCl, 2.9×10^{-3} $g{\cdot}L^{-1}$ Fe-EDTA, and 0.02 $g{\cdot}L^{-1}$ Karentol. The medium was sterilized via autoclaving at 120 °C for 1 h.

Experiments were conducted in 15 independent bubble-column photobioreactors, each with a working volume of 300 mL. Cultures were aerated continuously at a rate of 0.2 *v*/v/min using filtered air. To regulate pH, pure CO_2 was injected on-demand into the airstream before entering each reactor. Temperature control was achieved by stabilizing the environment of the culture chamber housing the reactors. Illumination was provided by overhead fluorescent lamps, which were automated to provide the requested irradiance. Dissolved oxygen was maintained at 100 % saturation through continuous air bubbling.

All experiments were performed in batch mode. For inoculation, a starter culture grown in Erlenmeyer flasks under continuous illumination (200 $\mu E{\cdot}m^{-2}{\cdot}s^{-1}$) was used. The inoculum volume was adjusted to 30 % of the total reactor volume at the beginning of each experiment. This strategy ensured a moderate initial biomass concentration, facilitating a robust assessment of the influence of specific cultivation parameters. Throughout the experiments, each reactor was monitored daily. Parameters recorded included biomass concentration (via gravimetric analysis or optical density), chlorophyll fluorescence (as a proxy for photosynthetic activity), and detailed morphological analysis using the Microdeep™ imaging system. The latter allowed real-time microscopic assessment of filament structure, length distribution, and integrity across all conditions tested.

2.2. Microfluidic microscope (Microdeep™)

The Microdeep™ apparatus is a state-of-the-art microfluidic microscope designed for high-resolution imaging and quantitative analysis of microalgae cultures (Fig. 1). Developed to facilitate real-time

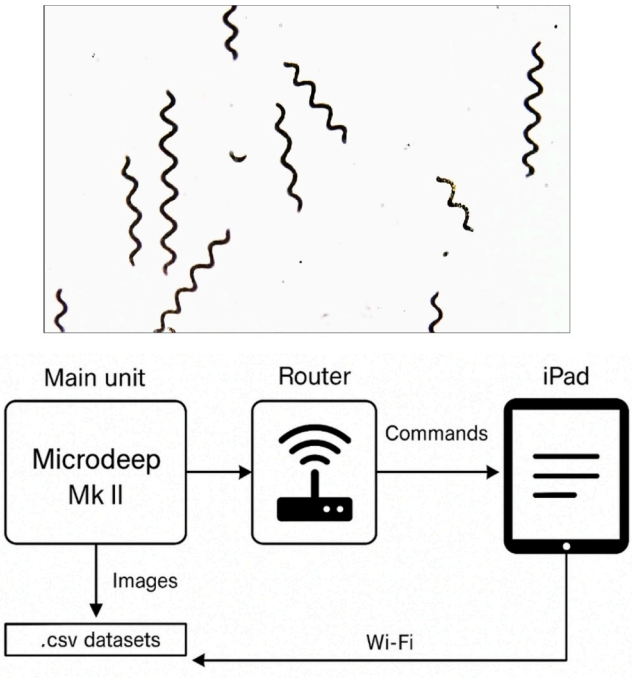

Fig. 1. Schematic representation and image capture example from the Microdeep™ system.

morphological monitoring, the system integrates a precision Olympus UPLFLN 20× objective lens, complemented by a blue excitation filter (UQG Optics, CM-500) and a linear polarizer (Thorlabs, LPVISE050-A). The core imaging operations are handled by the Microdeep™ Mk II platform, which captures and processes digital images through an iPad Air 5 interface using the dedicated Microdeep™ iPadOS application.

The fluidic network features a Y-shaped channel design with dual inlets: one delivering undiluted culture and another introducing distilled water for real-time dilution and rinsing of the fluidic system. These flows are driven by Gröthen G328 peristaltic pumps and merge into an Ibidi μ-Slide flow chamber with a channel depth of 0.4 mm, where imaging occurs under laminar flow conditions. The optical and fluidic integration allows non-invasive analysis of cells in motion, closely replicating in situ cultivation conditions.

An embedded AI model—based on the YOLOv5 object detection architecture [16] and trained on a curated dataset of *A. platensis* images—automatically detects individual filaments in brightfield images. The YOLOv5-based model was trained with more than 20,000 annotated *A. platensis* images and achieves optimal segmentation accuracy at filament concentrations between 4×10^7 and 5×10^8 filaments·L^{-1} (0.08–0.57 g·L^{-1} DW), a range in which real-time processing (≈12 fps) and minimal filament overlap are simultaneously ensured. For each bounding box, a binary mask is generated using Gaussian adaptive thresholding, enabling robust segmentation under variable illumination. Within each box, contours are extracted and only the largest contour is retained to represent the filament. Length and diameter are then derived from the contour's surface area and perimeter, assuming a constant cross-sectional diameter—a biologically valid approximation that introduces only minor errors over the length scale of interest. Notably, the image processing pipeline is optimized for real-time performance on iPadOS without relying on OpenCV, which was found to be too slow for embedded deployment.

Key outputs include filament concentration (filaments·mL^{-1}), length, diameter (μm), and dry mass equivalent (DME) in mg·L^{-1}. For accurate quantification, the system is calibrated using the K_{OO} parameter, a linear proportionality constant that compensates for depth-of-field limitations inherent to the microchannel geometry. This constant depends on both the object detection model and optical configuration and is determined through a three-point gravimetric calibration.

In order to assess the analyzed volume necessary for calculating the DME, two critical factors of the MicroDeep system were considered: the image area and the optical depth. Based on the calibrated conversion from pixels to microns, it is established that an image with dimensions 1600 × 1200 pixels corresponds to an area measuring approximately 1.432 mm^2 (1.158 pixels per micron). The depth of field associated with the objective lens utilized by the MicroDeep system is specified as 5.79 μm. To refine this value, it is adjusted using a correction coefficient (K_{OO}) that compensates for the optical constraints inherent in the microfluidic chamber. Upon applying this correction, the effective depth of field is determined, resulting in a final analyzed volume of approximately 0.0337 μL for each field of view captured in the image. To ascertain the concentration of filaments, which is expressed in units of filaments per litre, the procedure involves dividing the overall count of detected filaments by the comprehensive volume analyzed. This comprehensive volume is ascertained by multiplying the volume attributed to a single field by the total number of fields evaluated during the analysis process. The number of analyzed fields is automatically defined by the acquisition duration and flow rate, typically encompassing 100–300 sequential frames captured from the continuous laminar flow of the culture; hence, each field represents an independent time-step rather than a static region, ensuring statistical representativeness of the filament population. The resulting data are exported in high-resolution image formats and structured .csv files, enabling downstream statistical and morphological analyses.

3. Results and discussion

3.1. Use of Microdeep™ for dry biomass determination

Accurate determination of dry biomass is a fundamental parameter for the effective operation, monitoring, and optimization of microalgae cultivation systems, including those based on *A. platensis*. Biomass concentration is directly linked to productivity, culture health, and downstream processing efficiency [17,18]. Traditionally, dry weight is measured through gravimetric analysis, which involves filtration and oven-drying of culture samples. While this method is precise, it is time-intensive—requiring several hours to yield results—and unsuitable for rapid decision-making or real-time process control in dynamic cultivation environments [19]. To circumvent this limitation, fast optical methods such as spectrophotometry have become widely used to estimate biomass through absorbance or turbidity readings. However, these techniques are prone to inaccuracies due to their sensitivity to morphological variability, pigmentation levels, and cell aggregation, especially in filamentous species like *A. platensis* [12]. Consequently, continuous recalibration of correlation curves is necessary, undermining their robustness in automated systems.

In this context, the emergence of image-based biomass quantification platforms, such as Microdeep™, presents a promising alternative. These systems allow for the direct assessment of dry mass via real-time microscopic observation and AI-driven morphological analysis. In the present study, Microdeep™ was calibrated against conventional gravimetric measurements using a six-day batch culture of *A. platensis*. Each day, culture samples were analyzed by both gravimetric dry weight (DW) and optical DME, derived from Microdeep™, which uses a combination of optical density and filament morphology to compute Dry Mass Equivalent (g·L^{-1}). In practice, DME is derived from a hybrid optical–morphological algorithm that correlates image brightness with the total filament area and length obtained from segmentation, calibrated against gravimetric dry weight to correct for differences in filament structure and pigmentation. A key aspect of this calibration was determining the K_{OO} parameter, a corrective factor built into the Microdeep™ software to account for imaging distortions caused by the depth of the microfluidic chamber and object detection: this enables to discard out-of-focus filaments from the analysis. The calibration produced a highly linear relationship between DW and DME, described by the Eq. (1), with a K_{OO} value of 4.06 (Fig. 2). The derived linear regression exhibited an $R^2 > 0.99$, including for samples from a batch culture on which both growth rate and biochemical composition varies significantly, demonstrating agreement between Microdeep™ estimations and gravimetric standards.

$$DW = KOO_{OO} \cdot DME \quad (1)$$

The calibration was validated within a biomass concentration range of 0.08 to 0.57 g·L^{-1}, as determined by gravimetric analysis. Within this range, the DME estimated by the Microdeep™ system showed a strong linear correlation with actual dry weight measurements, ensuring high accuracy and reproducibility. For concentrations exceeding 0.57 g·L^{-1}, it is recommended to dilute the culture using the onboard microfluidic system to maintain measurements within the optical and analytical limits of the imaging setup. This validated range is highly relevant to practical microalgal cultivation scenarios. In large-scale production systems—particularly open raceway reactors, which dominate commercial *A. platensis* cultivation—typical steady-state biomass concentrations range from 0.3 to 0.8 g·L^{-1}, with reported peaks reaching up to 1.5 g·L^{-1} under optimal light and nutrient conditions [12,20]. Thus, the Microdeep™ platform effectively covers the operational range of most industrial-scale cultures, offering a robust tool for non-destructive, real-time biomass monitoring and control.

The integration of such image-based monitoring methods into open systems represents a significant step forward, given the inherent variability in environmental parameters affecting productivity. The capacity

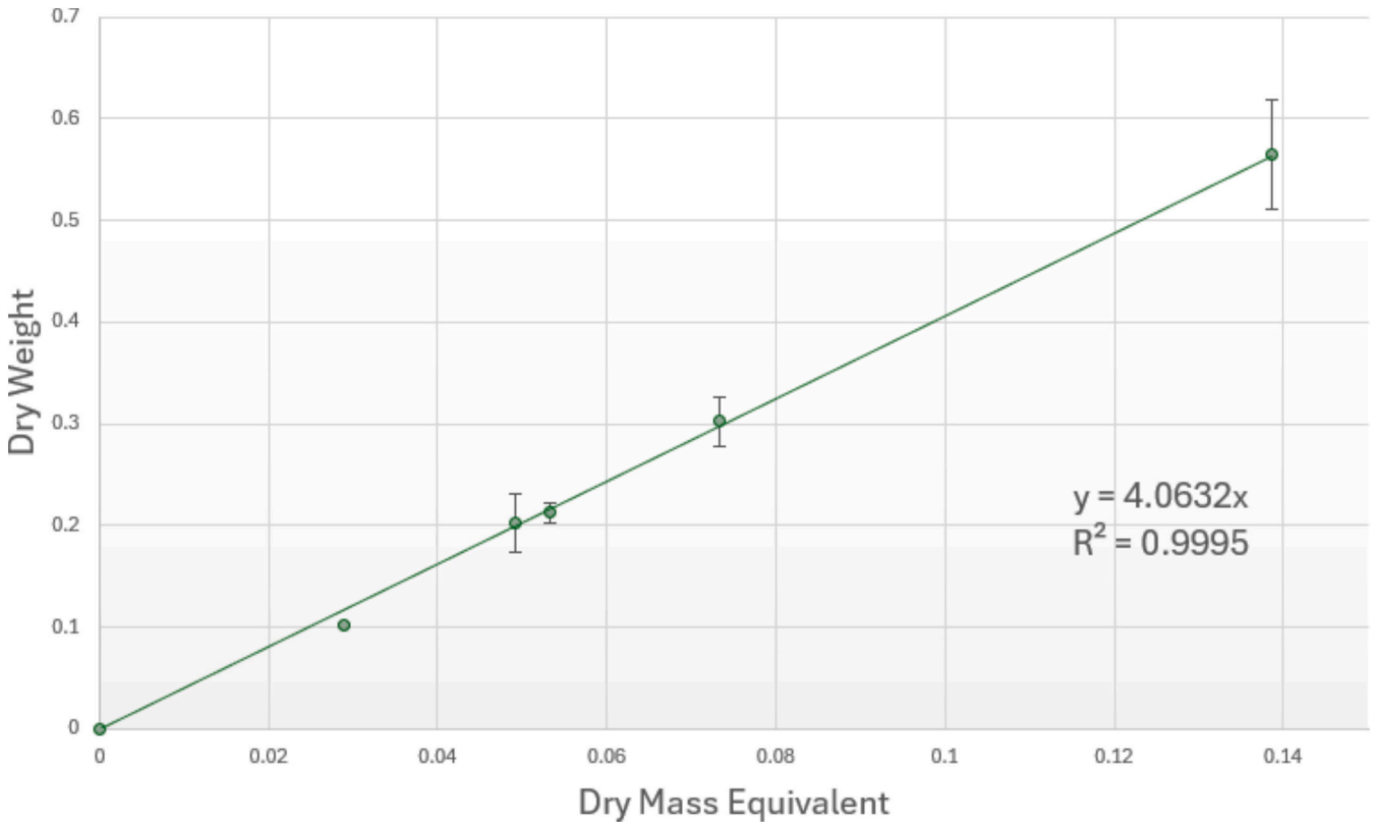

Fig. 2. Calibration of Microdeep™-derived Dry Mass Equivalent (DME) against gravimetric dry weight (DW). Measurements correspond to three replicates.

to rapidly detect deviations in biomass density without relying on time-consuming gravimetric techniques or less reliable spectrophotometry enhances process control and decision-making in commercial operations [17]. This confirms that Microdeep™ offers a fast, accurate, and non-destructive solution for biomass quantification—an advancement with substantial implications for automated photobioreactor control and bioprocess optimisation.

3.2. *Use of Microdeep™ for morphology characterization*

Beyond its validated utility for real-time dry weight estimation, the Microdeep™ system also enables advanced morphological profiling of filamentous *A. platensis*. This capability is critical for tracking structural adaptations and growth dynamics, particularly under varying cultivation conditions. In this study, Microdeep™ was employed to assess the morphological evolution of *A. platensis* over a six-day batch culture, providing quantitative insights into filament development and population dynamics. Filament lengths were sorted into 60 discrete classes, each spanning 10 μm wide, to cover the full range from 0 to 600 μm. This resolution permits statistically robust, population-wide assessments of morphological trends, enabling the identification of elongation phases, fragmentation events, and the formation of necridia—biological indicators of growth phase and culture health. Notably, this measured range aligns well with values reported in the literature, which describe *A. platensis* filaments as typically ranging from 50 to 500 μm in length and 6 to 12 μm in diameter [1,9,10]. Variations outside these bounds may reflect either extreme environmental stress or abnormal filament development, making continuous monitoring essential for bioprocess optimization.

Temporal evolution of filament length distribution in *A. platensis* during batch culture performed is showed in Fig. 3. At the beginning (0 h), the filament population displayed a uniform distribution across the analyzed length intervals, reflecting the homogeneous nature of the inoculum. Over the first 24–48 h, filament elongation remained limited, consistent with the lag phase typically observed in microbial systems as cells adapt to new nutrient and environmental conditions [11]. However, subtle increases in filament numbers within the 20–120 μm range were noted, attributable to early-stage binary fission events and the emergence of necridia—specialized breakage zones that promote filament segmentation [9,10]. These morphological processes signal the beginning of cellular acclimation and population expansion. During this period, a dynamic equilibrium began forming in the mid-length ranges (130–220 μm), where the influx of newly divided short filaments counterbalanced the outflux of elongating ones. This balance indicates active remodeling of the filament population, where structural expansion and fragmentation co-occur as key mechanisms governing population density and uniformity. These dynamics suggest that the filament population evolves through a non-linear interplay of growth and fragmentation, laying the foundation for a distribution-based modeling framework that captures the full morphological spectrum over time.

Between 48 and 72 h, a marked shift in the filament length distribution became evident, highlighting the onset of the exponential growth phase (Fig. 3). This phase was characterized by increased cellular division, robust metabolic activity, and a dual pattern of filament elongation and fragmentation. Notably, the proportion of filaments exceeding 220 μm surged early on but began to decline gradually after the 48-h mark. This decline suggests that elongated filaments underwent active segmentation via necridia, resulting in an increased presence of shorter filament classes. Such segmentation events play a critical role in the self-renewal and spatial optimization of the culture, facilitating better light penetration and nutrient access in dense systems [1]. By 96 to 144 h, the culture exhibited full exponential characteristics. Microdeep™ data revealed widespread filament proliferation across all length intervals, with the most significant expansion occurring in the shorter ranges (30–130 μm). The mean filament length decreased from an initial 146.8 μm to 124.98 μm by the end of the experiment, a trend directly linked to

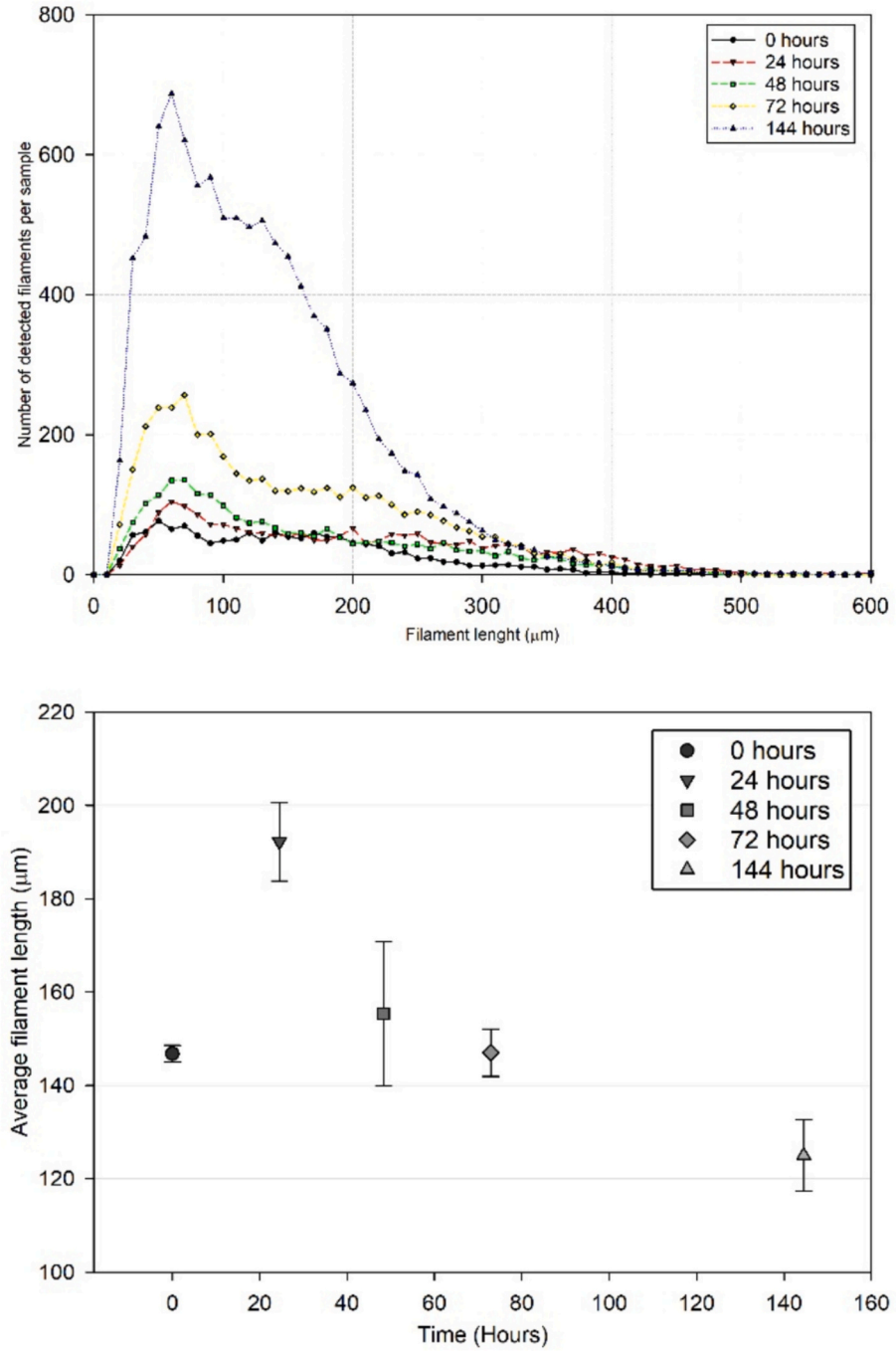

Fig. 3. Temporal variation in filament morphology during a six-day batch culture of A. platensis (0.018 mL sample was analysed in every time interval).

the ongoing generation of necridia and active binary fission. This reduction in average filament size may superficially resemble a stress response; however, in the context of batch growth under optimal conditions, it reflects a strategic biological adaptation aimed at enhancing cellular division rates and increasing population density.

From a biotechnological perspective, this pattern is highly desirable. Shorter filaments reduce the risk of shear damage during agitation, enhance homogeneity in suspension cultures, and improve harvesting efficiency during downstream processes such as filtration and centrifugation. Additionally, filament length modulation through necridia formation plays a key role in maintaining genetic stability and morphological resilience across generations [9,10]. The real-time monitoring capabilities of Microdeep™ were pivotal in capturing these dynamic shifts. Unlike traditional static microscopy or bulk optical density measurements, this system enabled continuous, non-destructive observation of filament population dynamics with submicron resolution and morphological specificity. These data not only validate the utility of Microdeep™ as a research and monitoring tool but also underscore the value of filament morphology as a quantitative biomarker for evaluating culture health, growth kinetics, and physiological responses.

3.3. Use of Microdeep™ to determine the influence of culture conditions on the performance of cultures

Following the successful validation of the Microdeep™ system as a reliable tool for quantifying biomass and assessing morphological traits in *A. platensis*, the platform was subsequently applied to evaluate the influence of environmental conditions on algal performance. This study

aimed to determine how variations in key cultivation parameters—specifically temperature, pH, irradiance, and agitation—impact both biomass productivity and filament morphology. Unless otherwise specified, all experiments were performed under baseline conditions of 25 °C, pH 10, irradiance 200 μmol·m^{-2}·s^{-1}, and moderate agitation (300 rpm), with only one parameter varied at a time to isolate its specific effect. A series of batch trials were conducted over a 24-h period. In each trial, one environmental variable was selectively modified while all others were held constant to isolate its specific effect on culture behavior. This design enabled a precise evaluation of how each parameter independently shaped the physiological and structural characteristics of *A. platensis*. Critical metrics such as filament count, filament length, and dry matter equivalent (DME) were continuously recorded using Microdeep™, allowing for dynamic monitoring of morphological adaptations and biomass accumulation.

Temperature trials were conducted across six setpoints—10, 15, 25, 35, 40, and 45 °C—under fixed pH (10) and irradiance (200 μmol·m^{-2}·s^{-1}). This range was chosen to encompass suboptimal, optimal, and inhibitory thermal environments. Literature suggests *A. platensis* achieves peak growth and productivity at 30–35 °C, with some strains tolerating up to 40 °C; productivity and phycocyanin yield notably decline beyond this optimal window [20,21]. pH trials were performed at 6, 8, 10, and 11, while maintaining temperature at 25 °C and irradiance at 200 μmol·m^{-2}·s^{-1}. Prior studies indicate that *A. platensis* thrives in alkaline conditions, with optimal growth typically occurring at pH 9–10, helping to suppress contaminant organisms and enhance pigment and biomass production; growth declines significantly below pH 8 or above pH 10.5 ([22]; Potts & Coleman, 2013). Light intensity trials ranged from 200 to 2200 μmol·m^{-2}·s^{-1}, simulating low to high irradiance environments while keeping temperature and pH constant. Optimal irradiance levels for *A. platensis* are reported between 100 and 300 μmol·m^{-2}·s^{-1}, favoring maximal biomass yield and pigment content; above 600 μmol·m^{-2}·s^{-1}, photoinhibition may occur [23,24]. Finally, agitation intensity was varied using magnetic stirrers between 300 and 1200 rpm. Adequate agitation ensures nutrient distribution and gas exchange, but excessive shear can damage filaments; typical systems maintain moderate shear to balance mixing and filament integrity [25].

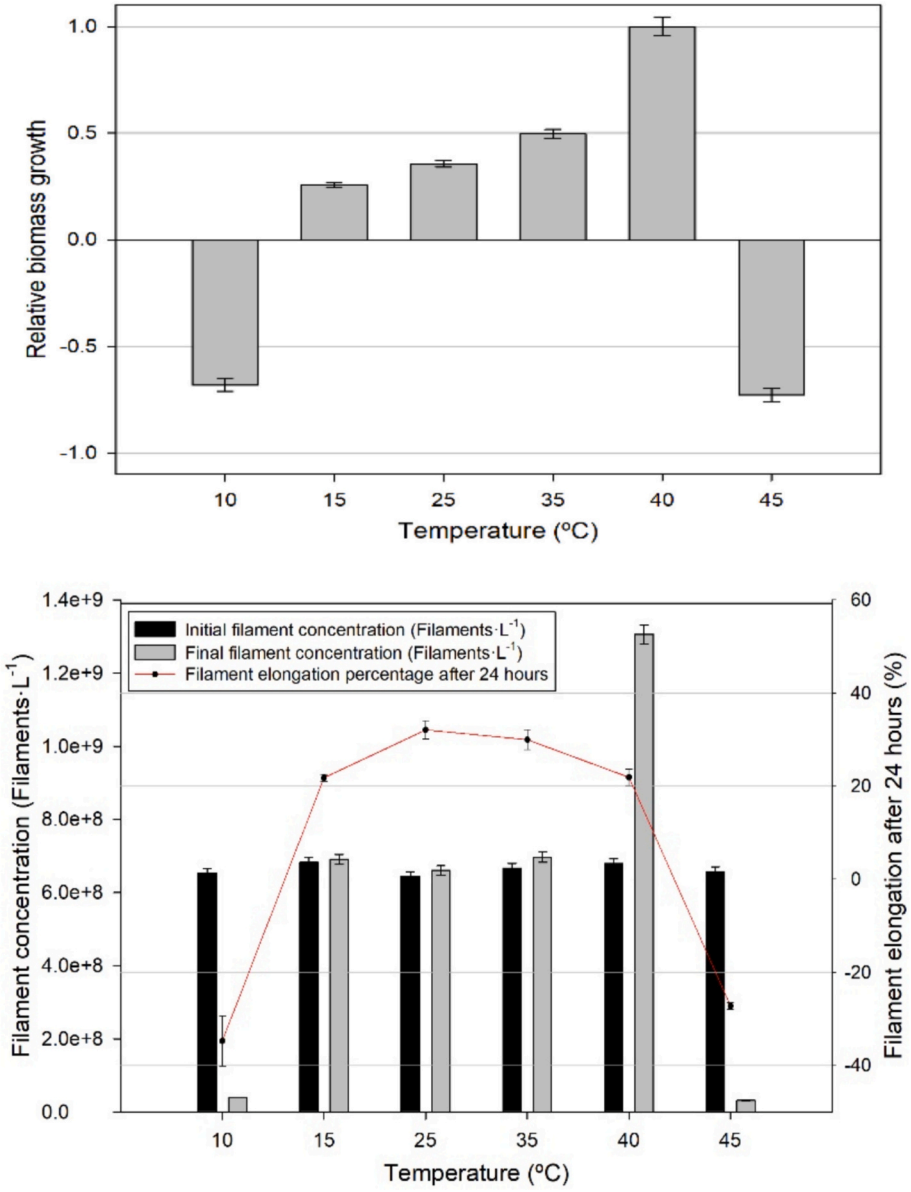

Fig. 4. Influence of temperature on A. platensis biomass productivity and morphology after 24 h.

3.4. Influence of temperature

Fig. 4 illustrates the influence of temperature on both biomass accumulation and filament morphology in *A. platensis* after 24 h of cultivation under standardized conditions of pH 10 and irradiance at 200 μmol·m^{-2}·s^{-1}. The data, generated using the Microdeep™ system, revealed that 40 °C yielded the highest increase in biomass concentration, affirming previous findings that *A. platensis* exhibits robust thermotolerance and maintains elevated metabolic activity under warm conditions [21]. At this temperature, filament count rose sharply from 6.78·10^{8}to 1.31·10^{9} filaments·L^{-1}, suggesting intense cellular division and filament fragmentation. Interestingly, although filament length also increased, this was not the most substantial elongation observed across the temperature range. This discrepancy indicates that the surge in population was driven by enhanced necridia formation, a known mechanism of filament segmentation that boosts culture density without necessarily increasing filament length [9]. Consequently, the average filament length rose by only 21.9 %, as the fragmentation process outpaced elongation.

In contrast, moderate increases in both biomass and filament length were recorded at 25 °C and 35 °C, aligning with prior literature that identifies these values as optimal or near-optimal for *A. platensis* growth [20]. Among these, 35 °C was particularly favourable, with relative biomass growth reaching 0.5, compared to 0.4 at 40 °C and 0.35 at 25 °C. These findings suggest that while 40 °C promotes rapid proliferation through necridia, 35 °C provides a more balanced environment that supports both filament elongation and stable biomass accumulation. Cultures subjected to 10 °C and 45 °C displayed marked reductions in both filament number and length. The final filament counts plummeted to 44,235 and 34,962, respectively, demonstrating that these thermal extremes lie outside the viable range for *A. platensis* and are associated with cellular stress or mortality [21]. From a morphological standpoint, filament elongation peaked at 25 °C and 35 °C, reaching 32.1 % and 30.0 %, respectively. These conditions likely minimized environmental stress, enabling uninterrupted filament development. Conversely, at 40 °C, elongation was suppressed, despite high filament numbers. This outcome is consistent with increased necridia production, which accelerates fragmentation and produces a higher proportion of shorter filaments, thereby lowering the average filament length despite overall population expansion [9].

These observations highlight the complex interplay between temperature, filament morphology, and biomass productivity in *A. platensis*, underscoring the need to tailor cultivation conditions based on the desired balance between cell density and filament structure.

3.5. Effect of pH

Fig. 5 illustrates the influence of pH on *A. platensis* growth, identifying a pH range of 8–10 as optimal for this strain. These results align with previous studies indicating that this interval provides near-ideal conditions for both biomass accumulation and structural robustness [1,11]. Outside this range, growth diminishes notably, reflecting the sensitivity of cyanobacterial physiology to pH deviations. At pH 6 and 11, growth rates decline significantly due to environmental stress. Specifically, at pH 11, the total filament count decreased markedly—by 4.9·10^{7} filaments per litre—suggesting high alkalinity impedes culture viability. This reduction is attributed to carbonate precipitation processes that cause flocculation and sedimentation, leading to partial loss of biomass [1]. Similar inhibitory effects have been documented in the literature for comparable alkaline pH levels [9].

Filament length data corroborate these growth trends. While most pH conditions resulted in unchanged or reduced filament lengths, pH 8 was an exception, showing significant filament elongation. Additionally, cultures at pH 6, 8, and 10 experienced net increases in total filament counts—1.1·10^{7}, 7.2·10^{6}, and 5.5·10^{6}filaments per litre, respectively—although the rise observed at pH 6 appears to derive primarily from filament fragmentation rather than true reproductive activity [9]. In contrast, the pH 11 condition, despite a marginal increase in biomass, displayed substantial physiological stress, consistent with high pH-induced precipitation effects [1].

Collectively, these findings reinforce the importance of maintaining cultivation pH between 8 and 10 to maximize productivity in *A. platensis*. Operating within this window supports healthy biomass yields, robust filament growth, and minimal stress-induced fragmentation, aligning with established guidelines for industrial microalgal production systems [1,11].

3.6. Effect of irradiance

Fig. 6 presents the experimental results evaluating the impact of varying irradiance levels on the biomass productivity and filament morphology of *A. platensis*. A clear trend emerged from the data: moderate light intensity, particularly at 200 μmol·m^{-2}·s^{-1}, promoted optimal physiological responses. This condition yielded the highest biomass accumulation, greatest filament count, and maximum filament elongation, indicating that this irradiance range facilitates both cellular proliferation and structural development in *A. platensis*. These findings are consistent with previous studies that have identified the optimal light range for *A. platensis* to lie between 150 and 200 μmol·m^{-2}·s^{-1}. Within this range, photosynthetic efficiency is maximized while minimizing the risk of photo-oxidative damage [10,26]. Notably, the cultures grown at 200 μmol·m^{-2}·s^{-1} also exhibited slightly darker pigmentation. This pigmentation shift may reflect elevated phycocyanin and chlorophyll content, typical indicators of optimal growth under non-stressful conditions [11].

From a morphological perspective, filament elongation was accompanied by structural regularity, and some filaments adopted a more linear shape, a behavior frequently observed during rapid growth phases [9]. From a morphological perspective, filament elongation was accompanied by structural regularity, and some filaments adopted a more linear shape—a qualitative observation consistently noted across replicates, although not quantitatively analyzed by the current image-processing algorithm. These structural changes suggest that under this irradiance, *A. platensis* maintains normal cell cycle progression and filament stability. Conversely, cultures exposed to excessive irradiance levels, up to 2200 μmol·m^{-2}·s^{-1}, demonstrated a pronounced decline in biomass productivity and filament integrity due to cellular disintegration and filament fragmentation, hallmarks of photoinhibition and oxidative stress [10]. Under such conditions, light absorption exceeds the capacity of the photosynthetic machinery, leading to reactive oxygen species accumulation and damage to photosystems.

3.7. Effect of agitation

To evaluate the mechanical resilience of *A. platensis* under varying agitation conditions, a series of short-term (3-h) batch culture experiments were conducted. Cultures were subjected to agitation speeds ranging from 300 to 1200 rpm, and morphological characteristics were monitored before and after treatment. A floating magnetic stirrer was employed to prevent filament trituration between the stirrer and the bottom of the reactor. Representative images and quantitative data are displayed in Fig. 7. Across all tested speeds, the cultures showed no visible signs of filament damage or morphological deformation. Filament counts, average lengths, and helical integrity remained consistent throughout the trials. These findings indicate that *A. platensis* can tolerate short-duration mechanical agitation up to 1200 rpm without undergoing structural compromise.

However, it is critical to recognize that rotational speed (rpm) alone is not the fundamental determinant of agitation-induced damage. Rather, the shear rate—a measure of the velocity gradient imposed on the fluid—is the primary factor influencing mechanical stress experienced by filamentous cyanobacteria. The shear rate is dependent not

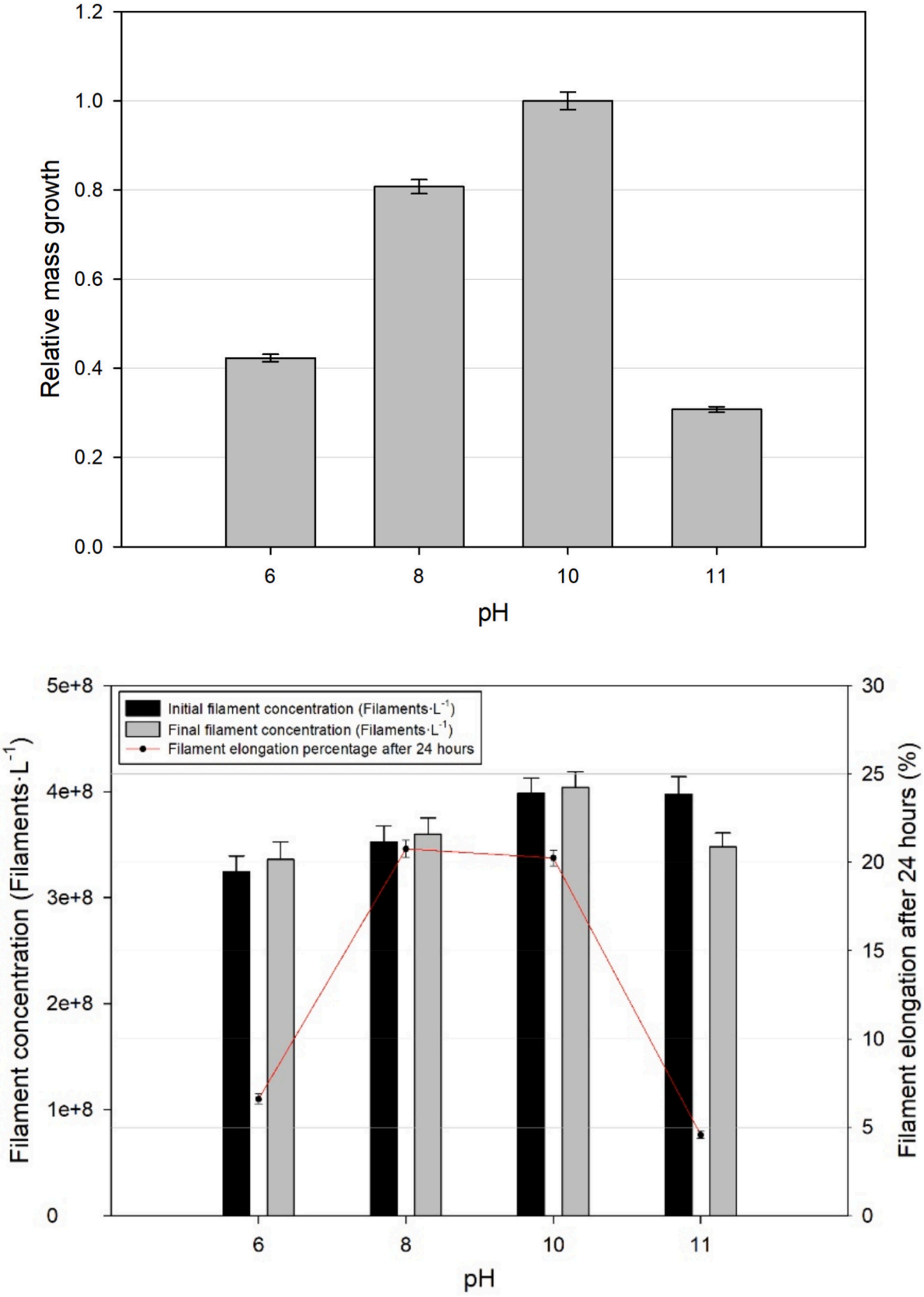

Fig. 5. Effect of pH on A. platensis growth and filament characteristics.

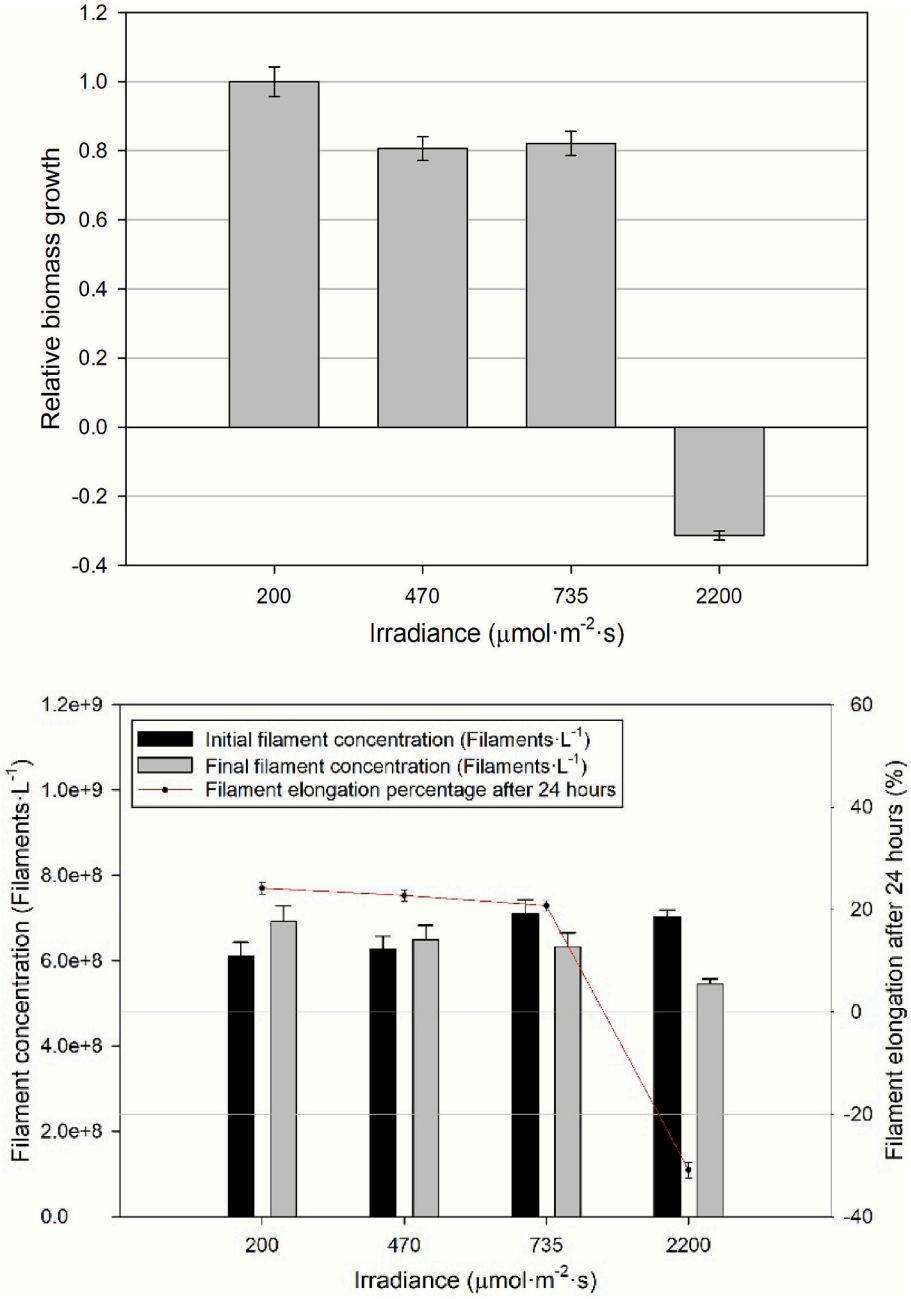

Fig. 6. Response of A. platensis to different irradiance levels over 24 h.

only on rpm, but also on reactor geometry, impeller design, fluid viscosity, and flow patterns [27]. For instance, a 1000 rpm setting in a narrow column reactor may generate significantly higher localized shear than the same setting in a wide-open raceway. This mechanistic distinction aligns with prior studies that documented morphological damage in *A. platensis* cultures exposed to high shear environments rather than high rpm per se. For example, Raoof et al. [28] demonstrated that impeller-induced shear could fragment filaments and suppress growth, particularly in vertical reactors where turbulence is concentrated. Similarly, Ismaiel et al. [11] observed pigment loss and cell deformation in cultures subjected to poorly distributed shear stress fields.

Therefore, for accurate process optimization, agitation protocols should be designed based on measured or modelled shear rates rather than on rpm alone. Tools such as viscometric analysis or computational fluid dynamics (CFD) simulations can be used to estimate shear profiles in various reactor configurations. This approach ensures that mixing efficiency is achieved without compromising filament integrity—especially critical in systems aiming for high biomass productivity and quality.

4. Conclusion

This study underscores the critical role of rapid, high-resolution monitoring in optimizing the cultivation of *A. platensis*. The Microdeep™ microfluidic platform proved effective for real-time quantification of both biomass concentration and filament morphology—two parameters essential for evaluating culture performance. The strong correlation between Dry Mass Equivalent (DME) and conventional dry weight measurements confirms its potential as a surrogate for continuous, non-invasive biomass estimation. More importantly, the system allowed detailed observation of morphological dynamics at the

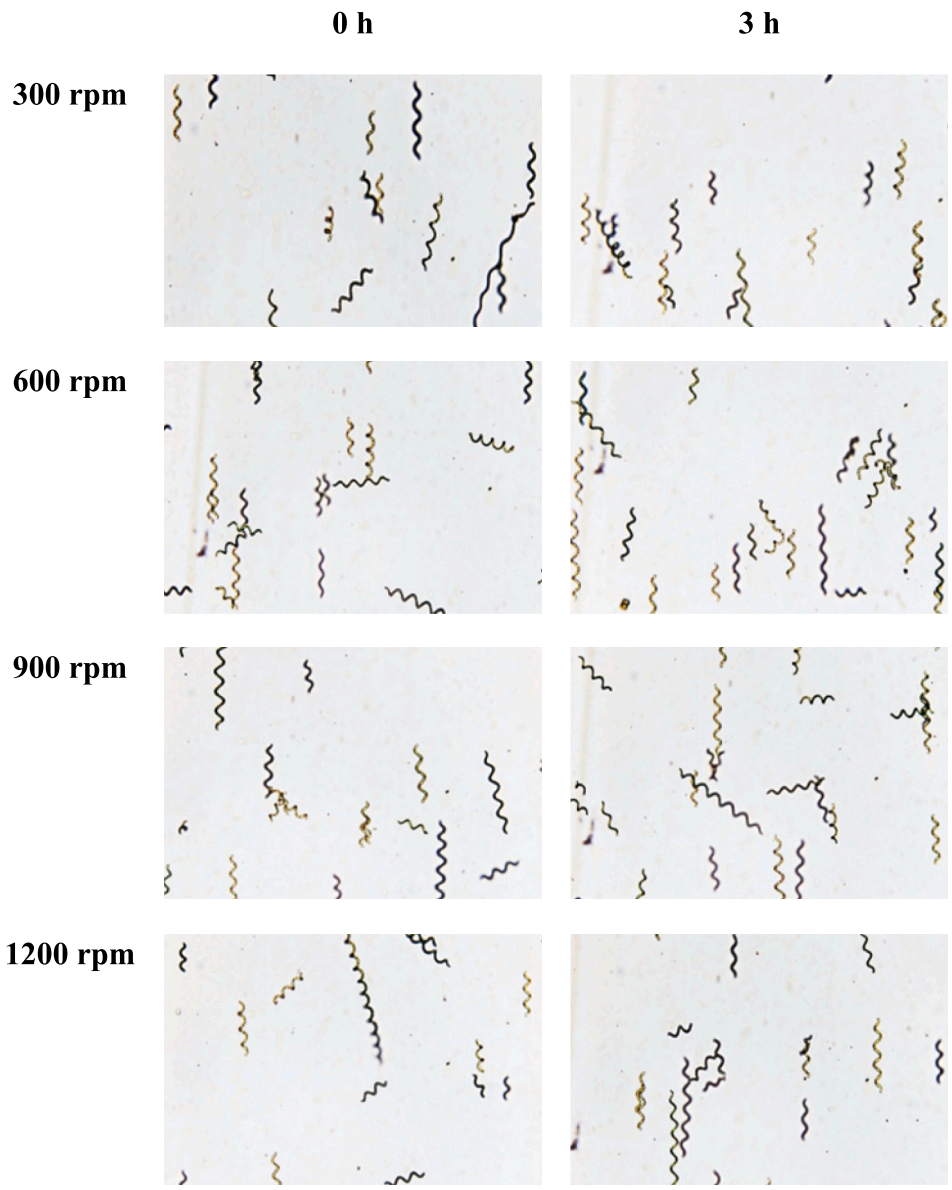

Fig. 7. Morphological stability of A. platensis under varying agitation intensities.

population scale, capturing transitions in filament length distributions, necridia formation, and fragmentation events that signal shifts in physiological status. These morphological changes, often invisible to bulk metrics like optical density, emerged as reliable indicators of environmental stress, reproductive activity, and overall culture health. This distribution-level insight opens new avenues for modeling the coupled dynamics of filament growth and breakage.

Experimental trials further revealed that culture conditions—specifically temperature, pH, and irradiance—significantly affect both biomass productivity and filament morphology. The optimal growth performance was observed at 40 °C and pH 10 under moderate irradiance (200 $\mu mol \cdot m^{-2} \cdot s^{-1}$), conditions that supported robust filament elongation and maximal biomass accumulation. In contrast, suboptimal conditions (e.g., pH 6, 11 or temperatures below 15 °C and above 45 °C) induced pronounced morphological alterations, such as increased filament breakage or shortened chain lengths, associated with reduced growth rates. These findings validate the use of filament morphology as a sensitive and early biomarker of culture performance. While agitation did not induce observable damage during short trials, more comprehensive studies are needed to evaluate long-term shear effects. Ultimately, this work demonstrates that combining rapid imaging-based diagnostics with controlled environmental adjustments enables more precise and responsive cultivation strategies for *A. platensis* in biotechnological systems. Real-time, continuous monitoring adds a critical dimension to bioprocess control, allowing early detection of deviations and supporting adaptive, high-yield cultivation strategies.

CRediT authorship contribution statement

R. Gomez Vico: Writing – original draft, Validation, Methodology, Investigation. **David-A. Mendels:** Writing – review & editing, Supervision, Software. **Agathe Nguyen:** Methodology, Formal analysis, Data curation. **M. Barceló-Villalobos:** Investigation, Formal analysis. **F.G. Acién:** Conceptualization, Supervision, Writing – review & editing.

Declaration of competing interest

The authors declare no known competing financial interests or personal relationships that could have influenced the work reported in this

manuscript.

This study was carried out as part of a collaborative research effort between the University of Almería and Zorth SARL, under the framework of publicly funded projects including CYAN2BIO (PID2021-126564OB-C31), REALM (Grant Agreement No. 101060991), and NIAGARA (Grant Agreement No. 101146861), supported respectively by the Spanish Ministry of Science and Innovation, and the European Union's Horizon Europe Programme.

All funding sources are transparently acknowledged. None of the funding agencies had any role in the study design, data collection, data interpretation, or the decision to submit this manuscript for publication.

Acknowledgements

This work is part of the R&D project CYAN2BIO PID2021-126564OB-C31 funded by MCIN/AEI and "ERDF" A way of making Europe. This work was also supported by the REALM (Grant agreement 101060991) and NIAGARA (Grant Agreement No 101146861) projects funded by Horizon Europe – the Framework Programme for Research and Innovation (2021–2027).

Data availability

Data will be made available on request.

References

[1] A. Belay, Biology and Industrial Production of Arthrospira (Spirulina), Wiley, 2013.
[2] F. Jung, A. Krüger-Genge, P. Waldeck, J.H. Küpper, Spirulina platensis, a super food? Journal of Cellular Biotechnology 5 (2019) 43–54.
[3] A.L. Lupatini, L.M. Colla, C. Canan, E. Colla, Potential application of microalga Spirulina platensis as a protein source, J. Sci. Food Agric. 97 (3) (2017) 724–732.
[4] D. Kurpan, A. Idà, F.G. Körner, et al., Long-term evaluation of productivity and harvesting efficiency of an industrial *Spirulina* production facility, Bioresour. Technol. Rep. 25 (2024) 101741.
[5] F. Guidi, Z. Gojkovic, M. Venuleo, P.A.C.J. Assunção, E. Portillo, Long-term cultivation of a native Arthrospira platensis (Spirulina) strain in Pozo Izquierdo (Gran Canaria, Spain): technical evidence for a viable production of food-grade biomass, Processes 9 (8) (2021).
[6] R.E.H. Olivera, U.A.Y. Pari, A.P.D. Gonza, J.C. Huamanga, D.P. Salazar, J.S. Flores, Cultivo de Arthrospira platensis (Spirulina) en fotobiorreactor tubular doblemente curvado a condiciones ambientales en el sur del Perú, Rev. Colomb. Biotecnol. 17 (2015) 143–150.
[7] P. Saranraj, S. Sivasakthi, *Spirulina platensis*—food for future: a review, Asian J. Pharm. Sci. Technol. 4 (1) (2014) 26–33.
[8] S. Lage, Z. Gojkovic, C. Funk, F.G. Gentili, Algal biomass from wastewater and flue gases as a source of bioenergy, Energies 11 (3) (2018) 664.
[9] P.W. Zhi, Y. Zhao, Morphological reversion of Spirulina (Arthrospira) platensis (Cyanophyta): from linear to helical, J. Phycol. 41 (2005) 622–628.
[10] C.H. Jung, S. Braune, P. Waldeck, J.H. Küpper, I. Petrick, F. Jung, Morphology and growth of *Arthrospira platensis* during cultivation in a flat-type bioreactor, Life 11 (6) (2021) 585.
[11] M.M.S. Ismaiel, Y.M. El-Ayouty, M. Piercey-Normore, Role of pH on antioxidants production by Spirulina (Arthrospira) platensis, Braz. J. Microbiol. 47 (2016) 298–304.
[12] M. Kumar, J. Kulshreshtha, G.P. Singh, Growth and biopigment accumulation of cyanobacterium Spirulina platensis at different light intensities and temperature, Braz. J. Microbiol. 42 (2011) 1128–1135.
[13] E. Manirafasha, T. Murwanashyaka, T. Ndikubwimana, N.R. Ahmed, J. Liu, Y. Lu, X. Zeng, X. Ling, K. Jing, Enhancement of cell growth and phycocyanin production in Arthrospira (Spirulina) platensis by metabolic stress and nitrate fed-batch, Bioresour. Technol. 255 (2018) 293–301.
[14] S.K. Ratha, P.H. Rao, K. Govindaswamy, R.S. Jaswin, R. Lakshmidevi, S. Bhaskar, S. Chinnasamy, A rapid and reliable method for estimating microalgal biomass using a moisture analyser, J. Appl. Phycol. 28 (2016) 1725–1734.
[15] R. Gomez Vico, M. David, M. Barceló-Villalobos, F.G. Acién, Morphological Response of Arthrospira Platensis to Cultivation Conditions Using a Microfluidic Microscope. Unpublished Manuscript, 2024.
[16] J. Redmon, S. Divvala, R. Girshick, A. Farhadi, You only look once: unified, real-time object detection, in: Proc. IEEE Comput. Soc. Conf. Comput. Vis. Pattern Recognit, 2016, pp. 779–788, https://doi.org/10.1109/CVPR.2016.91.
[17] T.M. Mata, A.A. Martins, N.S. Caetano, Microalgae for biodiesel production and other applications: a review, Renew. Sust. Energ. Rev. 14 (1) (2010) 217–232.
[18] A. Richmond, Q. Hu, Handbook of Microalgal Culture: Applied Phycology and Biotechnology, 2nd ed., Wiley, 2013.
[19] Y.K. Lee, H. Shen, Basic culturing techniques, in: Z. Cohen (Ed.), Single Cell Oils: Microbial and Algal Oils, AOCS Press, 2009, pp. 33–54.
[20] G. Torzillo, A. Vonshak, Environmental stress physiology, in: A. Richmond, Q. Hu (Eds.), Handbook of Microalgal Culture: Applied Phycology and Biotechnology, 2nd ed., Wiley, 2013, pp. 90–113.
[21] T. Nghinaunye, P. Waldeck, C.H. Jung, J.H. Küpper, F. Jung, S. Braune, Response of *Arthrospira platensis* to different temperatures regarding growth and biochemical composition, Clin. Hemorheol. Microcirc. 86 (1–2) (2024) 205–211.
[22] M.B. Kamalanathan, K. Ashok, J. Senthil, T. Kalaiyarasu, Effect of pH on Arthrospira platensis production, Braz. J. Microbiol. 47 (2020) 298–304.
[23] D. Nuriyah, Z. Hasan, A. Satya, C.W. Arief, Effect of light intensity on the performance profile of Spirulina platensis cultivated in FCB atmospheric photobioreactors, World Scientific News 197 (2024) 216–231.
[24] P. Pongtharangkul, T. Oomori, Influence of light intensity and photoperiod on energy efficiency of biomass and pigment production of Spirulina platensis, Oilseeds and Fats, Crops and Lipids 15 (1) (2008) 14–20.
[25] A.I. Barros, M.G. de Morais, S.M. da Silva, Harvesting techniques applied to microalgae: a review, Renew. Sust. Energ. Rev. 51 (2015) 183–189.
[26] A. Vonshak, G. Torzillo, Environmental stress physiology, in: A. Richmond (Ed.), Handbook of Microalgal Culture, Blackwell, 2004, pp. 57–82.
[27] H. Wang, W. Zhang, L. Chen, J. Wang, T. Liu, The influence of light and culture conditions on the growth and antioxidant content of Spirulina platensis, J. Appl. Phycol. 24 (6) (2012) 1537–1545.
[28] B. Raoof, B.D. Kaushik, R. Prasanna, Formulation of a low-cost medium for mass production of Spirulina, Biomass Bioenergy 30 (6) (2006) 537–542.